ЖЭТФ, 2004, том 126, вып. 5 (11), стр. 1267–1276

STATIC AND DYNAMIC CHARGE INHOMOGENEITY AND CRYSTAL-FIELD FLUCTUATIONS FOR $4f$ IONS IN HIGH-T_c CUPRATES

A. S. Moskvin**, Yu. D. Panov, N. V. Mel'nikova

Ural State University
620083, Ekaterinburg, Russia

Submitted 16 June 2004

The main mechanism of inhomogeneous broadening and relaxation of crystal-field excitations for rare-earth ions in cuprates is believed to be provided by the fluctuations of crystalline electric field induced by a static and dynamic charge inhomogeneity generic for the doped cuprates. Such an inhomogeneity is assumed to be a result of topological phase separation. We address the generalized granular model as one of the model scenarios to describe the static and dynamic charge ingomogeneity in cuprates. The charge subsystem is believed to be similar to that of the Wigner crystal with the melting transition and phonon-like positional excitation modes. We consider a simple model of charge inhomogeneity that allows us to elucidate the main universal features of the density of CF states and the respective inhomogeneous broadening. The formal description of R-ion relaxation mainly coincides with that of the recently suggested magnetoelastic mechanism by Lovesey and Staub.

PACS: 74.72.-h, 76.30.Kg, 78.70.Nx

1. INTRODUCTION

Inelastic neutron scattering (INS) spectroscopy is a powerful tool that allows unambiguously determining the Stark multiplet structure and crystal-field (CF) potential in rare-earth (R) based high-T_c superconducting materials such as $Y_{1-x}R_xBa_2Cu_3O_{6+y}$ [1, 2]. This technique provides detailed information on the electronic ground state of the R-ions, which is important to understand the thermodynamic magnetic properties and the observed coexistence between superconductivity and long-range magnetic ordering of the R-ion sublattice at low temperatures. Moreover, INS spectroscopy may be effectively used for a quantitative monitoring of the decay of the antiferromagnetic state of the parent compound and the evolution of the superconducting state upon doping, because the linewidths of CF transitions are believed to directly probe the electronic susceptibility. The relaxation behavior appears to be extremely dependent on the energy at which the susceptibility is probed. The crystal-field INS spectroscopy is widely used to reveal the opening of an electronic gap in the normal state of underdoped superconductors [1] and to examine its anisotropy [3, 4]. Recently, the Ho^{3+} CF-INS spectroscopy was used to investigate the oxygen and copper isotope effects on the pseudogap in the high-temperature superconductors Ho-124 and $(LaHoSr)_2CuO_4$ [5, 6]. But the mechanism of the relaxation of rare-earth ions in cuprates becomes the issue of hot debates [7, 8] that question the current interpretation of information detected by the INS spectroscopy.

In the normal state, the excited crystal-field levels of an R-ion interact with phonons, spin fluctuations, and charge carriers. These interactions limit the life-time of the excitation; thus the observed crystal-field transitions exhibit line broadening. Similarly to the case of the conventional Fermi-liquid metals, the interaction with the charge carriers is considered the dominating relaxation mechanism in cuprates. This interaction is usually assumed to be an isotropic exchange coupling with the effective spin Hamiltonian $H_{ex} = -2I(g_J - 1)(\mathbf{s} \cdot \mathbf{J})$, where I is an exchange integral that should be nearly independent of the particular R-ion under consideration, g_J is the Lande factor, $\mathbf{s}$ is the spin moment of a charge carrier, and $\mathbf{J}$ is the total momentum of the R-ion. Such a scenario seems to

*E-mail: alexandr.moskvin@usu.ru

be rather natural if the predominant spin channel of neutron scattering is taken into account. The detailed theory of the respective relaxation mechanism was developed by Becker, Fulde, and Keller (BFK-model) [9]. The corresponding intrinsic linewidth appears to increase almost linearly with temperature ($\Gamma(T) \propto \rho^2 T$) according to the well-known Korringa law [10]. Here, ρ is the coupling constant, $\rho = I(g_J - 1)N(E_F)$, where $N(E_F)$ is the density of states (DOS) at the Fermi level. The deviation from a linear temperature dependence at low temperatures has been usually interpreted in terms of the opening of a (pseudo)gap and the associated reduction in damping. Fitting the high-temperature linewidth data in the framework of the simple or modified Korringa law, one obtains the coupling constant values that typically vary from 0.003 to 0.006 [1, 3–6].

We emphasize that the spin channel of relaxation directly implies the relevance of the Fermi-liquid scenario for cuprates, with many signatures of non-Fermi-liquid behavior ignored. However, the spin-exchange model has a number of visible inconsistencies, firstly as concerns the magnitude of the coupling constant. Indeed, a linear temperature dependence of the relaxation time above T_c observed in EPR studies of S-ion Gd^{3+} in $YBa_2Cu_3O_7$ after Korringa fitting yields the magnitude of the exchange integral $I \approx 3 \cdot 10^{-4}$ eV (Ref. [12]), which directly points to unrealistically big values of the spin coupling constants ρ found in all the INS experiments on CF transitions. Some problems exist with the Lande factor scaling proportional $(g_J - 1)$. In studying the system $Y_{1-x}R_xBa_2Cu_3O_{6+y}$ (R = Er, Ho, Tm), Mukherjee et al. [11] found $|\rho(\mathrm{Tm})/\rho(\mathrm{Ho})| \approx 2$ instead of the theoretically expected value $(g_{\mathrm{Tm}} - 1)/(g_{\mathrm{Ho}} - 1) = 2/3$, and $|\rho(\mathrm{Tm})/\rho(\mathrm{Er})| \approx 4.5$, instead of the expected $(g_{\mathrm{Tm}} - 1)/(g_{\mathrm{Er}} - 1) = 5/6$. This clear disagreement evidences against the exchange mechanism. The spin-exchange scenario fails to explain the «strange» doping dependence of Tm^{3+} relaxation in Tm-123 [13] and Nd^{3+} relaxation in $(LaSrNd)_2CuO_4$ [14].

Finally, Staub et al. [15] have found that the Lorentzian linewidth of the quasi-elastic neutron scattering for Tb^{3+} in $YBa_2Cu_3O_7$ can be properly described by the simple $(\exp(\Delta/k_BT) - 1)^{-1}$ law typical of the Orbach processes governed by lattice vibrations. They have shown that such an interpretation also describes the results obtained earlier for Ho^{3+} and Tm^{3+}. They conclude that the interactions with the charge carriers are negligible and that the interactions with the lattice vibrations are responsible for the relaxation behavior of the $4f$ electrons in cuprates. Therefore, the INS results that claim to probe the superconducting gap or the pseudo-gap should be reexamined in terms of Orbach processes. A similar conclusion was drawn in [14] for Nd^{3+} relaxation in $(LaSrNd)_2CuO_4$. Lovesey and Staub [16] have shown that the dynamic properties of the lanthanide ions (Tb^{3+}, Ho^{3+}, and Tm^{3+}) are adequately described by a simple three-state model, not unlike the one introduced by Orbach for the interpretation of electron paramagnetic resonance signals from a lanthanide ion in dilute concentration in a salt. The cross section for inelastic scattering of neutrons by the lanthanide ion is derived by constructing a pseudospin $S = 1$ model and treating the magnetoelastic interaction as a perturbation on the three crystal-field states. The scattering of neutrons is thus a quasielastic process and the relaxation rate is proportional to $(\exp(\Delta/k_BT) - 1)^{-1}$, where Δ is the energy of the intermediate crystal-field state at which the density of phonon states is probed. However, this very attractive scenario also faces some visible difficulties with the explanation, for instance, of the unusual nonmonotonic temperature dependences and too large oxygen isotope effect in the INS spectra of Ho-124 and Ho-214 systems [5, 6] some doping dependences in Y-123 and Nd-214 systems [14]. The origin of the anomalously large low-temperature inhomogeneous broadening remains unclear. The magnetoelastic mechanism yields very small magnitudes of $\Gamma(T = 0)$, one or two orders smaller than that found in experiment.

Comparing two mechanisms, we underline their difference that seems to be of primary importance: the spin-channel mechanism takes the fluctuations of the effective magnetic field on R-ion into account, while the phonon (magnetoelastic) mechanism deals with fluctuations of the electric field. Moreover, the conventional spin-channel mechanism actually probes spin fluctuations rather than charge fluctuations, although its contribution to the linewidth $\Gamma(T) \propto (I\,N(E_F))^2$ is believed to strongly depend on the density of carriers. However, this relationship is derived in the framework of the Fermi-liquid scenario, and is to be modified if one addresses the typical antiferromagnetic insulating state. Interestingly, in Refs. [8, 15, 16], the phonon (magnetoelastic) mechanism is addressed as an alternative to the charge fluctuations. As an example, the authors point to insulating materials where «... the density of carriers is essentially zero...» [8], which forbids the charge fluctuation channel of relaxation.

We emphasize that both groups of researchers underestimate the role of the conventional spinless charge fluctuation channel. Indeed, the CF Hamiltonian for an R-ion in cuprate can be written in its standard form as

$$H_{CF} = \sum_{k=2,4,6} \sum_{-k \le q \le k} B^*_{kq} \hat{O}^q_k,$$

where $\hat{O}^q_k$ are Stevens equivalent operators, $B_{kq} = b_{kq}\langle r^k \rangle \gamma_k$, where b_{kq} are CF parameters, $\gamma_2 = \alpha$, $\gamma_4 = \beta$, $\gamma_6 = \gamma$ (α, β, γ are Stevens parameters), and

$$b_{kq} = \langle b_{kq} \rangle + \Delta b_{kq},$$

which may be expressed within the well-known point-charge model as

$$\Delta b_{kq} = \sum_i \frac{q C^k_q(\mathbf{R}_i)}{R^{k+1}_i} (\hat{n}_i(t) - \langle n_i \rangle),$$

where C^k_q is the tensorial spherical harmonics and $\hat{n}_i(t)$ is the charge number operator. Conventional metals are characterized by a very short-time charge dynamics, which allows neglecting the contribution of charge fluctuations to the inhomogeneous broadening and relaxation of R-ions in the low-energy range of CF energies, and considering a mean homogeneous charge distribution. An altogether different picture emerges in the case of cuprates where we deal with various manifestations of static and dynamic charge inhomogeneity (see, e.g., Refs. [17, 18] and references therein). Moreover, the INS spectroscopy of CF excitations itself yields an impressive picture of charge inhomogeneity in the 123 system [1, 2], where it was found that the observed CF spectra separate into different local components whose spectral weights distinctly depend on the doping level, i.e., there is clear experimental evidence for cluster formation. The onset of superconductivity can be shown to result from percolation, which means that the superconductivity is a property of inhomogeneous materials. It seems probable that the dynamical rearrangement of the charge system at the temperatures above T_c somehow affects both the inhomogeneous broadening of CF transitions and R-ion relaxation.

2. CHARGE INHOMOGENEITY IN CUPRATES: TOPOLOGICAL PHASE SEPARATION

At present, the stripe model of inhomogeneity [18] is most popular in cuprate physics. It is worth noting that this model is based on the more universal idea of topological phase separation, with the doped particles assumed to localize inside the domain walls of a bare phase.

Below, we address one of the topological phase separation scenarios that may be termed a generalized granular model for doped cuprates. We assume that the CuO_2 layers in parent cuprates may gradually lose their stability under electron/hole doping, while a new self-organized multigranular 2D phase becomes stable.

The new scenario implies that the unconventional phase state evolves from parent insulating cuprate as a result of self-trapping of the charge transfer excitons (CT) accompanied by a self-consistent lattice polarization and the appearance of the «negative-U» effect. Parent insulating cuprates appear to be unstable with regard to self-trapping of the low-energy one- and two-center CT excitons [19, 20] with a nucleation of electron–hole (EH) droplets being actually the system of coupled electron CuO_4^{7-} and hole CuO_4^{5-} centers glued in the lattice due to strong electron–lattice polarization effects. Such a system can be regarded as an electron–hole Bose liquid described by the generalized Bose–Hubbard Hamiltonian. Doping, or deviation from half-filling in the EH Bose liquid is accompanied by formation of multicenter topological defects such as charge-order (CO) bubble domain(s) with Bose superfluid (BS) and extra bosons localized in domain wall(s), or a topological CO+BS phase separation, rather than uniform mixed CO+BS supersolid phase [21, 22]. Such a situation partly resembles that of granular superconductivity.

The most probable possibility is that every micrograin accumulates one or two particles. Then the number of such entities in a multigranular texture nucleated with doping has to depend on the doping nearly linearly. Generally speaking, each individual micrograin may be characterized by its position, nanoscale size, and the orientation of the U(1) degree of freedom. In contrast with the uniform states, the phase of the superfluid order parameter for a micrograin is assumed to be unordered. The granular structure must be considered largely dynamic in nature.

In the long-wavelength limit, the off-diagonal ordering can be described by an effective Hamiltonian in terms of the U(1) (phase) degree of freedom associated with each micrograin. Such a Hamiltonian contains a repulsive, long-range Coulomb part and a short-range contribution related to the phase degree of freedom. The latter term can be written in the form of a so-called Josephson coupling, standard for the XY model,

$$H_J = -\sum_{\langle i,j \rangle} J_{ij} \cos(\varphi_i - \varphi_j), \qquad (1)$$

where φ_i and φ_j are global phases for micrograins centered at the respective points i and j, and J_{ij} is the Josephson coupling parameter. The Josephson coupling gives rise to the long-range ordering of the phase of the superfluid order parameter in such a multi-center

texture. Such a Hamiltonian represents a starting point for the analysis of disordered superconductors, granular superconductivity, and insulator–superconductor transition with an $\langle i,j\rangle$ array of superconducting islands with phases φ_i, φ_j.

To account for the Coulomb interaction and allow for quantum corrections, we introduce the charging energy [23]

$$H_{ch} = -\frac{1}{2}q^2 \sum_{i,j} n_i (C^{-1})_{ij} n_j$$

into the effective Hamiltonian, where n_i is the number operator for particles bound in the ith micrograin; it is quantum-mechanically conjugate to φ, $n_i = -i\partial/\partial\varphi_i$, $(C^{-1})_{ij}$ is the capacitance matrix, and q is the particle charge.

Such a system appears to reveal a tremendously rich quantum-critical structure [24, 25]. In the absence of disorder, the $T = 0$ phase diagram of the multigranular system implies either triangular or square crystalline arrangements with a possible melting transition to a liquid. We note that the analogy with the charged $2D$ Coulomb gas implies the Wigner crystallization of the multigranular system with a Wigner crystal (WC) to the Wigner liquid melting transition. Naturally, additional degrees of freedom of the micrograin provide a richer physics of such lattices. For a system to be an insulator, disorder is required that pins the multigranular system and also causes the crystalline order to have a finite correlation length. The traditional approach to Wigner crystallization implies the formation of a WC for densities lower than the critical density, when the Coulomb energy is greater than the kinetic energy. The effect of quantum fluctuations leads to a (quantum) melting of the solid at high densities or at a critical lattice spacing. The critical properties of a two-dimensional lattice without any internal degrees of freedom are successfully described by applying the BKT (Berezinsky–Kosterlitz–Thowless) theory to dislocations and disclinations of the lattice. This description proceeds in two steps. The first step implies the transition to a liquid-crystal phase with a short-range translational order, and the second involves the transition to isotropic liquid. In such a system, if the micrograin positions are fixed at all temperatures, the long-wavelength physics is described by an (anti)ferromagnetic XY model with expectable BKT transition and a gapless XY spin-wave mode.

The low-temperature physics in a multigranular system is governed by an interplay of two BKT transitions, for the U(1) phase and the positional degrees of freedom, respectively [25]. Dislocations lead to a mismatch in the U(1) degree of freedom, which makes the dislocations bind fractional vortices and leads to a coupling of translational and phase excitations. The BKT temperatures either coincide (square lattice) or the melting one is higher (triangular lattice) [25].

Quantum fluctuations can substantially affect these results. Quantum melting can destroy the U(1) order at sufficiently low densities where the Josephson coupling becomes exponentially small. A similar situation is expected to occur in the vicinity of structural transitions in a multigranular crystal. With increasing the micrograin density, the quantum effects result in a significant decrease of the melting temperature compared with the classical square-root dependence. The resulting melting temperature can reveal an oscilating behavior as a function of the particle density with zeros at the critical (magic) densities associated with structural phase transitions.

In terms of our model, the positional order corresponds to an incommensurate charge density wave, while the U(1) order corresponds to superconductivity. In other words, we arrive at a subtle interplay between two orders. The superconducting state evolves from a charge order with $T_C \leq T_m$, where T_m is the temperature of the melting transition, which could be termed the temperature of the opening of the insulating gap (pseudo-gap!?).

The normal modes of a dilute multigranular system include the pseudo-spin waves propagating inbetween the micrograins, the positional fluctuations, or quasiphonon modes, which are gapless in a pure system but are gapped when the lattice is pinned, and, finally, fluctuations in the U(1) order parameter.

The orientational fluctuations of the multigranular system are governed by the gapless XY model [24]. The relevant model description is most familiar as an effective theory of the Josephson junction array. An important feature of the model is that it displays a quantum critical point.

The low-energy collective excitations of a multigranular liquid includes the usual longitudinal acoustic phonon-like branch. The liquid crystal phases differ from the isotropic liquid in that they have massive topological excitations, i.e., disclinations. We note that liquids do not support transverse modes, and these could survive in a liquid state only as overdamped modes. It is therefore reasonable to assume that solidification of the bubble lattice is accompanied by stabilization of transverse phonon-like modes with their sharpening below the melting transition. In other words, the instability of transverse phonon-like modes signals the onset of melting. The phonon-like modes

in the bubble crystal have much in common with the usual phonon modes, but because of the electronic nature they can hardly be detected by inelastic neutron scattering.

A generic property of the positionally ordered bubble configuration is the sliding mode, which is usually pinned by the disorder. The depinning of sliding mode(s) can be detected in a low-frequency and low-temperature optical response.

We note that as regards the CF fluctuations, there is no principal difference between the contributions of real phonon modes and quasiphonon modes of a multigranular system. Moreover, it is worth noting that the charge inhomogeneity in a multigranular system is proned to be closely coupled with lattice structural distorsions. However, stabilization of transverse phonon-like modes in multigranular system that accompanies its solidification at the temperatures above T_c may strongly affect the CF relaxation due to a mechanism identical to the magnetoelastic mechanism proposed by Lovesey and Staub. In a sense, such a conclusion reconciles the «old» spin-fluctuation [1, 2] and the «new» magnetoelastic phonon [15, 16] approaches to the INS spectroscopy of cuprates with R-ions.

Above, we addressed a simplified model of «rigid» bubbles and neglected any possible internal or conformational degree of freedom. However, the bubble can actually be characterized by a subtle interplay of orbital degrees of freedom with a pseudo-Jahn–Teller effect. In other words, we may anticipate a set of different conformational states of the bubble.

3. CHARGE INHOMOGENEITY AND INHOMOGENEOUS LINE BROADENING OF CF TRANSITIONS IN CUPRATES

Neutron spectroscopy involves energies of several meV and is therefore susceptible to dynamical effects of the order of 10^{-13} s. All the slower processes contribute to the inhomogeneous broadening of CF transitions. The effects of inhomogeneous line broadening are clearly seen for the crystal field excitation in $Ho_{1-x}Y_xBa_2Cu_3O_7$ with the energy near 0.5 meV [4]. Although the CF transition is between two singlets, it reveals an intrinsic multiple-peak structure at low temperatures, comprising a dominant central peak with shoulders on each side, and a tail on the higher energy side. The key assumption on which the traditional analysis is based is that the observed line shape arises from rare-earth ions distributed in slightly different local environments, but subject to the same relaxation processes. In other words, one assumes that the observed line shape reflects a temperature-independent inhomogeneous broadening and a universal temperature-dependent relaxation mechanism. The spectrum measured at a particular temperature is then given by the convolution of a broadening function characteristic of that temperature and the residual line shape at absolute zero. Hence, the relaxation is assumed to be described by a single broadening function whose position, width, and amplitude depend on the temperature. However, this approach fails to explain an unusual low-temperature line shape of the CF transition with an unexpectedly large ($\Gamma_0 \approx 0.2$ meV) residual linewidth of the central peak. The low-temperature experimental spectra are likely to reveal some sort of continuous distribution of crystal fields, rather than a simple superposition of only three components whose spectral weights distinctly depend on the doping level, as was assumed in Refs. [1, 2].

In the continuum approximation, the resultant CF transition line shape in the static case corresponds to the density of the local CF distribution convoluted with the individual line shape. The density of the local CF distribution has a number of universal features typical of a rather wide range of inhomogeneous 2D potentials. Under certain conditions, we can easily predict the character and number of such peculiarities in the complex structure of the CF transition and even the line shape itself.

A. Simple point charge model of electron inhomogeneity

To make our consideration more quantitative, we consider a simple model of charge inhomogeneity centers organized into an incommensurate square superlattice in the CuO_2 plane with a parameter a, and hypotetical R-ions with the momentum $J = 1$ positioned above (under) the CuO_2 plane (the z-coordinate in units of a: $z = Z/a$), as in the R-123 structure, and having the $M = 0$ ground singlet state. In the approximation of a strong tetragonal CF component, $|B_0^2| \gg |B_2^2|$, the energies of two excited states with $|M| = 1$ are shifted by

$$\Delta E_{\pm}(x,y) \propto \left[\sqrt{\frac{3}{2}}\Delta B_0^2(x,y) \pm |\Delta B_2^2(x,y)|\right].$$

Hence, we can introduce two energy surfaces $E_{\pm}(x,y)$, where x and y are the plane coordinates of a rare-earth ion. The surfaces osculate at points with the tetragonal symmetry. The point-charge model for the CF parameters $B_{0,\pm 2}^2$ allows us to easily compute these surfaces.

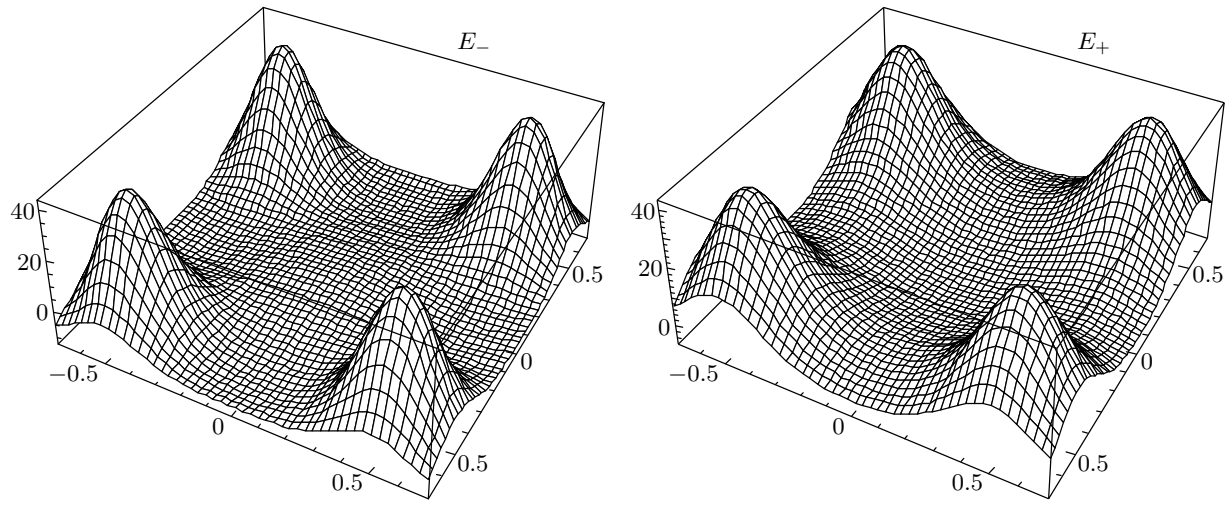

Fig. 1. Energy surfaces $E_\pm(x, y)$ for a model doublet ($z = 0.3$)

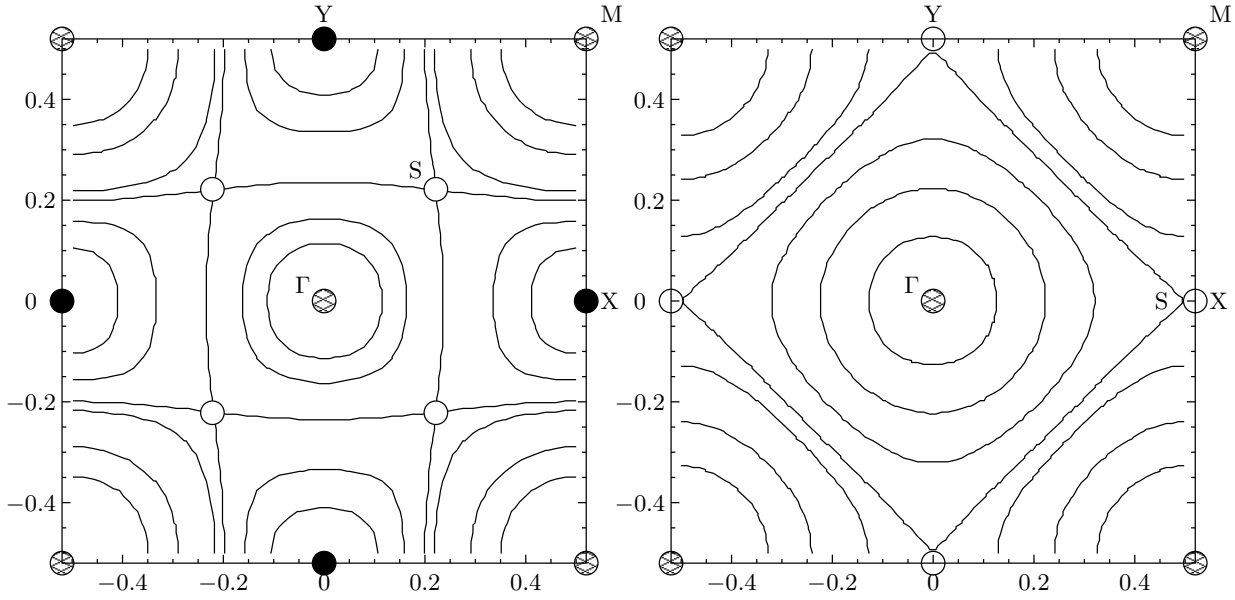

Fig. 2. Specific points in the elementary cell of incommensurate superstructure. Singular points and some isoenergetic curves for the $E_-(x, y)$ (left-hand side) and $E_+(x, y)$ (right-hand side) branches of a model doublet (see text for details)

For $z = 0.3$, they are shown in Fig. 1. At first sight, these surfaces differ insignificantly, but the isoenergetic curves reveal the distinction. In Fig. 2, we marked different singular points and some isoenergetic curves for both modes $E_\pm(x, y)$. Four points of type M at the corners of the square cell with the tetragonal symmetry correspond to sharp maxima of both $E_-(x, y)$ and $E_+(x, y)$. The Γ point at the center with the tetragonal local symmetry corresponds to a smooth local maximum of the energy $E_-(x, y)$ and a minimum of the energy $E_+(x, y)$. Four minima of $E_-(x, y)$ are situated at the points X(Y) on the boundaries where the $E_+(x, y)$ surface has saddle points. The saddle points of the $E_-(x, y)$ surface are situated inside the elementary cell. By varying the lattice separation, we may simulate the effect of varying the concentration of charge inhomogeneity centers. The energy surfaces $E_\pm(x, y)$ can be described by the density of states (DOS) defined as $\rho(E) \propto [dE/dS]^{-1}$, where $S(E)$ is the area of the cross section $E(x, y) = E = \text{const}$. The R-ions are assumed to be uniformly distributed in the x, y plane, and their number is proportional to the cross section area:

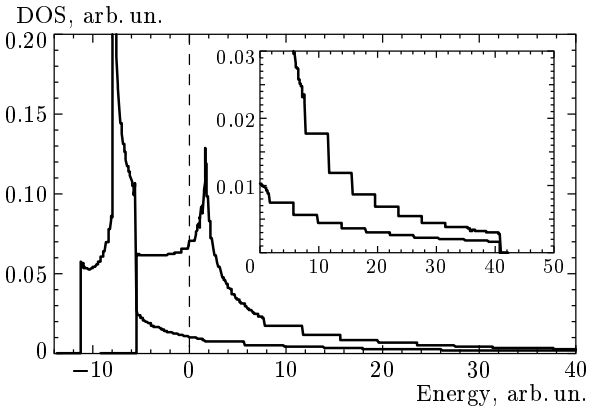

Fig. 3. Results of a numerical calculation of the density of states for the lower and upper branches $E_{\pm}(x, y)$ of a model doublet with $z = 0.3$

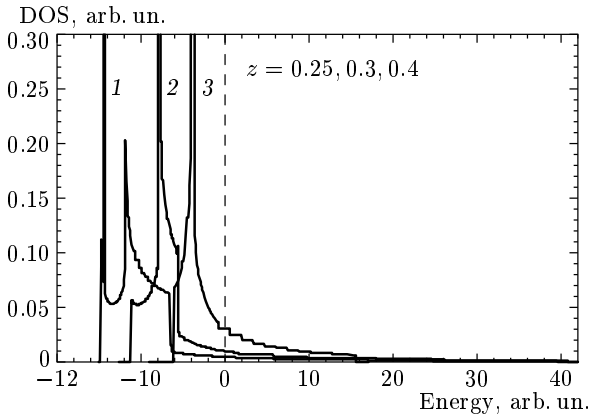

Fig. 4. Results of a numerical calculation of the density of states for the lower branch $E_{-}(x, y)$ of a model doublet for different values of the z parameter: $z = 0.25$ (*1*); 0.3 (*2*); 0.4 (*3*)

$dN_R(E) = \rho(E)dE \propto dS(E)$. The DOS has several singularities associated with extremal points (minima, maxima, and saddle points). The saddle points are of primary importance because they are known to yield a logarithmic divergence of the DOS in two-dimensional systems. Near the minima and maxima, the $E(S)$ dependence can be approximated as $E(S) \approx E(0) + aS^n$. It is clear that for $n \leq 1$, the density of states is finite at the extremum point, while for $n > 1$, it diverges at the extremum point. It is worth noting that sharp extrema with small n correspond to a small DOS. It is interesting to note a strong resemblance of the procedure to that for the conventional two-dimensional band model, where one deals with a **k**-momentum space.

The results of numerical calculation of the DOS for both the low-energy $|-\rangle$ and high-energy $|+\rangle$ modes are shown in Fig. 3.[1)] The inset in Fig. 3 shows the fine structure of the DOS near the maximum of the energies $E_{\pm}$. The dotted line shows the energy position of the $|\pm\rangle$ doublet failing the inhomogeneity potential. We note that both DOS's reveal the features typical of two-dimensional systems. This figure yields a nice illustration of the effects of charge incommensurability, in particular, the splitting effect resulting from local breaking of the tetragonal symmetry. It is worth noting that our model DOS obeys the a^{-3} scaling law.

Figure 4 shows the effect of varying the distance z of the R-ion from the CuO_2 plane. We see the change of the DOS shape with an expected narrowing and blue shift for larger z.

Our model approach yields a simple illustration of the concentration effects. Indeed, if we assume the generic square lattice for the inhomogeneity centers, we obtain a simple relation between the lattice parameter and concentration: $a^2 \propto 1/x$. Hence, given a fixed absolute magnitude of the Z parameter, we see that the dimensionless parameter $z = Z/a$ varies with the concentration of the charge inhomogeneity centers. In other words, Fig. 4 with additional a^{-3} scaling corrections yields an example of a change in the DOS with a rise of concentration. As expected, the rise of concentration results in a smoothing of the energy surfaces with a narrowing of the energy distribution and a sizeable shift of the main peak. Positional disorder due to conventional defects such as substituted ions, unconventional topological defects such as dislocations and disclinations (which are inherent for two-dimensional materials, however), and slow positional motion of bubbles result in an inhomogeneous broadening, which implies a weighted superposition of different energy surfaces $E(x, y)$. Such a broadening can be easily taken into account if we simply assume the Gaussian distribution of different $E(x, y)$ values near a mean value $\langle E(x, y)\rangle$. An illustrative example of a Gaussian broadening is shown in Fig. 5, where we have included both raw numerical data and the results of a convolution with the Gaussian function with the half-width $\gamma = 0.1, 0.5$.

Fast positional motion of the charge inhomogeneity centers results in averaging the crystal field potential acting on the R-ion. The simplest model of such an averaging in the framework of the point charge approximation for our square superlattice assumes the distribution of the point charges near mean positions **R** with the probability $W(\rho) \propto e^{-\rho^2/\langle\rho^2\rangle}$, where ρ

[1)] The numerical calculations were performed by E. Zenkov.

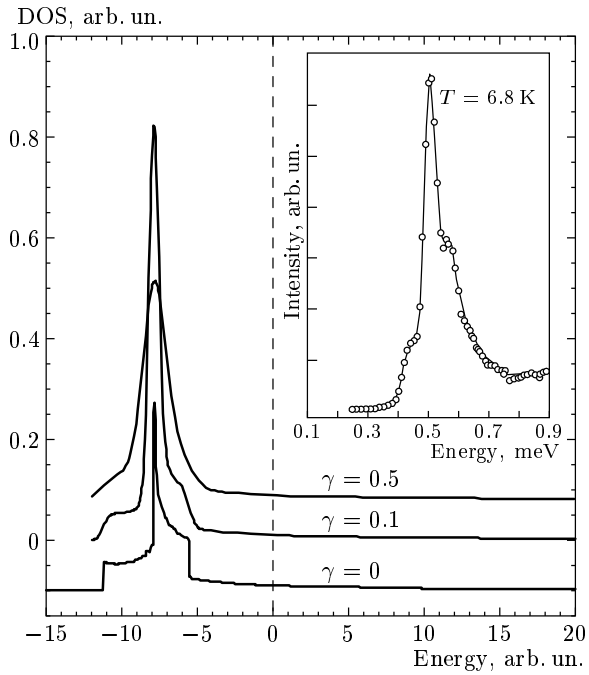

Fig. 5. Inhomogeneous broadening of the model CF transition. The results of a Gaussian convolution of the calculated DOS. The inset shows the experimental inelastic neutron scattering spectra of the ground state to the first excited state CF transition of Ho^{3+} in $Ho_{0.1}Y_{0.9}Ba_2Cu_3O_7$ in the energy range 0.1 to 0.9 meV [4]

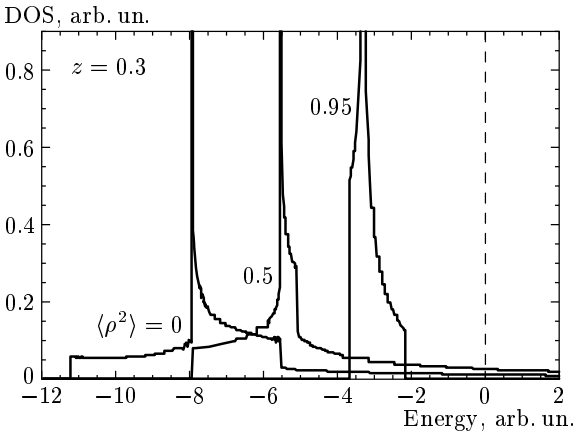

Fig. 6. Results of a numerical calculation of the density of states for the lower branch $E_-(x, y)$ of a model doublet given different values of the $\langle\rho^2\rangle$ parameter: 0; 0.5; 0.95

specifies the displacement from the mean position and $\langle\rho^2\rangle$ is a mean-square displacement. In general, the mean-square displacement is believed to be strongly anisotropic, with the predominant in-plane component. For simplicity, however, the numerical calculations of the energy surfaces $E_\pm$ were performed with an isotropic displacement. The averaged potential differs from the bare Coulomb potential in that it has smoothed and lower maxima, and hence the bounds of the DOS spectra shrink with a simultaneous shift of the center of gravity to higher energies (see Fig. 6). Interestingly, the shift of the center of DOS gravity is very sensitive to the z-component of the charge displacement and in a sense can be used as its measure.

However, this is not the only effect of averaging. As the extremum regions of $E_\pm(r)$ become flatter and their areas extend, the contribution of a greater number of adjacent sites to the extrema becomes important, each of them coming with its own phase. This leads to the specific interference phenomena. In particular, as the dispersion $\langle\rho^2\rangle$ increases, the extremum points of $E_\pm$ reveal a clear tendency to splitting. For example, the maximum of the bare E_- surface at the Γ point splits into four maxima, shifted towards the four corresponding M points, while a shallow minimum appears at the Γ point. Thus, unexpectedly enough, averaging can result in some complication of the energy surfaces in general. The same effect is obtained alternatively by increasing the z parameter.

As the charge distribution in the CuO_2 plane becomes more uniform, the $E_\pm$ energy separation progressively vanishes, because the potential of a uniformly charged plane yields no electric field gradient. This may be achieved either by increasing z or by amplifying fluctuations of the in-plane sites. Then the energy spectrum of the model consists of the $M = 0$ singlet ground state and the $M = \pm 1$ doublet, and the DOS spectrum of the only excited state reduces to a δ-peak that resides at zero energy in the adopted units. The numerical results (see Figs. 4 and 6) confirm this conclusion.

To summarize, the analysis of the real-space charge inhomogeneity makes it possible to approach the interpretation of the typical features of experimental spectra from a novel angle in terms of the «real-space DOS» singularities, which reflect some essential topological properties of the inhomogeneity-induced spatial distribution of the relevant physical parameters such as the crystal field for R-ions. The basic properties of these DOS singularities (their number, kinds, etc.) are rather stable against variations in the charge distribution and admit a simple classification scheme. For example, extremum points of the distribution correspond to jumps in the DOS spectra, while saddle points give rise to

sharp divergencies that manifest themselves as spectral peaks. The observed experimental spectrum should be regarded as a convolution of an individual line profile, the intensity factor, and the DOS function, contributing together to a complex resultant line shape. However, it is sometimes possible to discriminate between different sources of the spectral features. In particular, the proposed DOS mechanism is to be addressed in the case of «extra lines», where the number of spectral features observed exceeds that predicted from symmetry considerations.

B. Implications for CF transitions in cuprates

In the inset in Fig. 5, we present the low-temperature crystal field excitation spectrum in $Ho_xY_{1-x}Ba_2Cu_3O_7$ ($x = 0.1$) with the energy near 0.5 meV [4]. It may be concluded that the spectrum exhibits all the features found in our model simulation, and hence precisely the inhomogeneous broadening governs the line shape. The central peak seems to reflect the contribution of «saddle-point» R-ions, while the left-hand and right-hand side shoulders are associated with the R-ions exposed to the extremal CF magnitudes.

Bubbles in a crystal or liquid state of the cuprate participate in both slow and fast motion, and we should therefore expect a rather complicated interplay of inhomogeneous broadening and averaging/narrowing, which can strongly depend on the temperature. Simple classical considerations imply the T-linear high-temperature dependence of both $\langle\rho^2\rangle$ and the concentration of the topological defects in the bubble system such as dislocations and disclinations. However, the low-temperature behavior of $\langle\rho^2\rangle$ is governed mainly by quantum effects. It is worth noting that the contribution of topological defects changes when crossing the BKT transition temperature, which is accompanied by binding/unbinding of topological defects and the change in the behavior of correlation functions. At a first glance, the rise in the temperature has to suppress the inhomogeneous broadening due to a faster motion of bubbles. However, we actually deal with two competing T-dependent effects: the rise of the concentration of topological defects on the one hand and the rise of their mean velocity on the other.

Slow conformational motion can be described in terms of a finite diffusion, resulting in a linear-in-T dependence of the respective inhomogeneous broadening. Actually, we deal with a combined effect of different sources of static and dynamic factors governing the line shape of CF transitions. Its separation requires both further experimental information and a refinement of theoretical models.

4. CONCLUSIONS

We have argued that the main mechanism of inhomogeneous broadening and relaxation of crystal-field excitations for rare-earth ions in cuprates can be provided by the fluctuations of the crystalline electric field induced by a static and dynamic charge inhomogeneity generic for the doped cuprates. Such an inhomogeneity is assumed to be a result of topological phase separation. We have considered the generalized granular model as one of the model scenarios to describe the static and dynamic charge ingomogeneity in cuprates. The charge subsystem is believed to be similar to that of a Wigner crystal with the melting transition and phonon-like positional excitation modes. We have considered a simple model of charge inhomogeneity organized into an incommensurate square superlattice; this model allows elucidating the main universal features of the real-space density of CF states. It is worth noting that both static and dynamic effects are cosidered on an equal footing. We see that the studies of line narrowing for CF transitions for $4f$ ions in high-T_c cuprates provides an informative tool to investigate the charge rearrangement accompanying the onset of high-T_c superconductivity. Our model approach based on the analysis of the real-space DOS can be easily generalized to study other manifestations of the electron inhomogeneity in cuprates such as an inhomogeneous broadening of NMR-NQR signals.

This paper was supported in part by the INTAS (grant № 01-0654), CRDF (grant № REC-005), RME (grants № E 02-3.4-392 and № UR.01.01.062), and RFBR (grant № 04-02-96077). A. S. M. has benefited from stimulating discussions with A. T. Boothroyd, A. Mirmelstein, and J. Mesot.

REFERENCES

1. J. Mesot and A. Furrer, J. Supercond. **10**, 623 (1997).
2. J. Mesot and A. Furrer, in *Neutron Scattering in Layered Copper-Oxide Superconductors*, ed. by A. Furrer, Kluwer, Dordrecht (1998), p. 335.
3. J. Mesot, G. Böttger, H. Mutka, and A. Furrer, Europhys. Lett. **44**, 498 (1998).
4. A. T. Boothroyd, A. Mukherjee, and A. P. Murani, Phys. Rev. Lett. **77**, 1600 (1996).

5. D. Rubio Temprano, J. Mesot, S. Janssen, K. Conder, A. Furrer, H. Mutka, and K. A. Müller, Phys. Rev. Lett. **84**, 1990 (2000).

6. D. Rubio Temprano et al., Phys. Rev. B **66**, 184506 (2002).

7. A. T. Boothroyd, Phys. Rev. B **64**, 066501 (2001).

8. S. W. Lovesey and U. Staub, Phys. Rev. B **64**, 066502 (2001).

9. K.W. Becker, P. Fulde, and J. Keller, Z. Physik B **28**, 9 (1977).

10. J. Korringa, Physica C **16**, 601 (1950).

11. A. Mukherjee, A. T. Boothroyd, D. McK. Paul, M. P. Sridhar Kumar, and M. A. Adams, Phys. Rev. B **49**, 13089 (1994).

12. D. Shaltiel, C. Noble, J. Pilbrow, D. Hutton, and E. Walker, Phys. Rev. B **53**, 12430 (1996).

13. R. Osborn and E. A. Goremychkin, Physica C **185–189**, 1179 (1991).

14. M. Roepke, E. Holland-Moritz, B. Büchner, H. Berg, R. E. Lechner, S. Longville, J. Fitter, R. Kahn, G. Coddens, and M. Ferrand, Phys. Rev. B **60**, 9793 (1999).

15. U. Staub, M. Gutmann, F. Fauth, and W. Kagunya, J. Phys.: Condens. Matter **11**, L59 (1999).

16. S. W. Lovesey and U. Staub, Phys. Rev. B **61**, 9130 (2000).

17. J. Burgy, M. Mayr, V. Martin-Mayor, A. Moreo, and E. Dagotto, Phys. Rev. Lett. **87**, 277202 (2001).

18. E. W. Carlson, V. J. Emery, S. A. Kivelson, and D. Orgad, E-print archives, cond-mat/0206217.

19. A. S. Moskvin, R. Neudert, M. Knupfer, J. Fink, and R. Hayn, Phys. Rev. B **65**, 180512(R) (2002).

20. A. S. Moskvin, J. Málek, M. Knupfer, R. Neudert, J. Fink, R. Hayn, S.-L. Drechsler, N. Motoyama, H. Eisaki, and S. Uchida, Phys. Rev. Lett. **91**, 037001 (2003).

21. A. S. Moskvin, I. G. Bostrem, and A. S. Ovchinnikov, JETP Lett. **78**, 772 (2003).

22. A. S. Moskvin, Phys. Rev. B **69**, 214505 (2004).

23. S. A. Kivelson and B. Z. Spivak, Phys. Rev. B **45**, 10490 (1992).

24. A. G. Green, Phys. Rev. B **61**, R16299 (2000).

25. C. Timm, S. M. Girvin, and H. A. Fertig, Phys. Rev. B **58**, 10634 (1998).